

# Planar mapping of the liquid fraction of froth using ultrasound

## Flächige Darstellung des Wassergehaltes von Schaum mittels Ultraschall

Hannes Emmerich<sup>1</sup>, Leon Knüpfer<sup>2</sup>, Pavel Trtik<sup>3</sup>, Kerstin Eckert<sup>2,4</sup>, Sascha Heitkam<sup>2,4</sup>, Eric Starke<sup>5</sup>, David Weik<sup>1</sup>, Lars Büttner<sup>1</sup>, Jürgen Czarske<sup>1</sup>

<sup>1</sup>Technical University Dresden, Laboratory of Measurement and Sensor System Techniques, 01069 Dresden, Germany

<sup>2</sup>Helmholtz-Zentrum Dresden-Rossendorf, Institute of Fluid Dynamics, 01328 Dresden, Germany

<sup>3</sup>Paul Scherrer Institut, Laboratory for Neutron Scattering and Imaging, 5232 Villigen, Switzerland

<sup>4</sup>Technical University Dresden, Institute of Process Engineering and Environmental Technology, 01069 Dresden, Germany

<sup>5</sup>SICK Engineering GmbH, Bergener Ring 27, 01458 Ottendorf-Okrilla, Germany

### Kurzfassung

Flotationsprozesse sind essentielle Verfahren zur Ressourcenseparierung, deren Überwachung Unmengen an Wasser und Energie einsparen kann. Um sie zu steuern ist eine Messung der vorhandenen Phasenanteile des Schaums nötig. Derzeit existiert keine geeignete Messmethode die ohne Weiteres in den bisherigen Prozess integrierbar ist und eine Eindringtiefe von mehr als 5 cm besitzt. In dieser Arbeit stellen wir deshalb ein Messsystem zur Bestimmung der Flüssigkeitsverteilung im Schaum mit Hilfe von Ultraschall dar. Um der stark dämpfenden Wirkung des Schaums auf den Ultraschall entgegen zu wirken, nutzen wir niederfrequente Sonden mit einer Mittenfrequenz von 135 kHz. Elektroden bestimmen durch Leitfähigkeitsmessung einen integralen Wassergehalt. Innerhalb eines Flüssigkeitsbereichs von  $0,17...0,82 \cdot 10^{-2}$  wurde das Messsystem für eine Eindringtiefe von 9,2 cm zunächst kalibriert und durch eine simultane Neutronenbildgebung validiert. Eine absolute und relative Messunsicherheit von  $0,23 \cdot 10^{-2}$  und 42,5% war das jeweilige Resultat. Eine Auflösung von 7,5 mm in axialer, 13 mm in lateraler Richtung und 1 Hz in der Zeit wurde erreicht. In einem dynamischen inhomogenen Fall wurde das Messsystem zusätzlich für den Anwendungsfall validiert. Diese Untersuchung stellt einen ersten Schritt zur Prozessoptimierung in Flotationsprozessen dar.

### Abstract

Flotation processes are essential processes for resource separation, the monitoring of which can save vast amounts of water and energy. To control them, it is necessary to measure the phase fractions present in the froth. Currently, no suitable measurement method exists that can be easily integrated into the existing process and has a penetration depth of more than 5 cm. Therefore, in this paper we present a measurement system for determining the liquid distribution in foam using ultrasound. To counteract the strong attenuating effect of the foam on the ultrasound, we use low-frequency probes with a center frequency of 135 kHz. Electrodes determine an integral liquid fraction by conductivity measurement. Within a liquid range of  $0.17 \cdot 10^{-2}$  to  $0.82 \cdot 10^{-2}$ , the measurement system was first calibrated for a penetration depth of 9.2 cm and validated by simultaneous neutron imaging. An absolute and relative measurement uncertainty of  $0.23 \cdot 10^{-2}$  and 42.5 % was the respective result. A resolution of 7.5 mm in the axial, 13 mm in lateral direction and 1 Hz in time were obtained. In a dynamic inhomogeneous case, the measurement system was additionally validated for a use case. This investigation represents a first step towards process optimization in flotation processes.

## 1 Introduction

The upcoming change of the energy sector towards renewable energies requires an increase in extraction and processing of rare earth elements. One major process to separate valuable minerals from valueless gangue material is froth flotation. The ore is grinded to sub-millimetric particles which are added to the flotation cell. Suspensions of water and particles are enriched by at least two surfactants. One enables the suspension to foam up and one controls the hydrophobicity of the suspended particles. Injected air creates bubbles that collect hydrophobic particles, rise to the top and gather at the top of the cell and form an over-

flowing froth layer. In particular, the liquid fraction of the froth is a key parameters as it influences the rheology and stability of the froth. [1]

For such process control, innovative sensor concepts for the froth zone are required because currently no industrial sensor can provide information on the froth composition from below the froth surface. Approaches by optical means get limited by the opaqueness of the foam and provide only surface information. [2] Conductive measurements have by now only been used to achieve an integrated information about the foams liquid fraction. [3] By means of magnetic resonance measurement foam's liquid fraction for a range of 31 mm has been analyzed with a

spatial and temporal resolution of  $312\mu\text{m}$  and 2 s respectively. [4] Neutron imaging was able to achieve a spatial resolution of  $200\mu\text{m}$  for a 3 mm thick cuvette filled with foam within one second. [5] Anyhow, this measurement equipment can not be easily integrated into running industrial processes. Ultrasound in a low frequency range ( $< 200\text{ kHz}$ ) has shown to penetrate foam for several centimeters, even though the multiple phases of the foam attenuate the signal strongly. [6] We therefore build a measurement system consisting of multiple ultrasound transducers and electrodes that is able to calculate the liquid fraction distribution in two spatial dimensions over time.

## 2 Measurement System

Six ultrasound transducers ('Type S7' of the SICK Engineering GmbH, Ottendorf-Okrilla, Germany) with a mid frequency of  $135\text{ kHz}$  were stacked vertically as shown in Fig. 1. They have a diameter of  $13\text{ mm}$  and a vertical distance of  $13\text{ mm}$  to each other. Air matching production of the transducers and an upstream resonance circuit enable a desired input of energy in the system to be measured. In between the transducers electrodes with the dimensions  $9 \times 25\text{ mm}$  are positioned. This setup was embedded in a cylinder with a diameter of  $100\text{ mm}$ . On the opposing side two transmission transducer of the same type and three further electrodes were positioned vertically in an alternating order. In one pulse echo step, two ultrasound transducers emit a signal simultaneously by an excitation of  $\pm 84\text{ V}$  for five pulses. A neighbouring third transducer records the echo (RX-E-transducer) and the closest opposing TX-transducer (RX-T-transducer) records the transmitted signal. In the present measurements the pulse repetition frequency was set to  $60\text{ Hz}$  and ten RX-signals were averaged to improve the signal to noise ratio (SNR). A scan consisted of a sequential measurement of the ultrasound transducers. After every transducer of the six was used once as a RX-E-transducer the scan is complete.

Simultaneously to the 10 emitted US-signals, a  $1\text{ kHz}$  signal was applied to one electrode aside of the receiving echo-transducer and the closest one on the opposing side. The electrodes measure the integrated liquid fraction. [3] They are steered by an upstream multiplexer to measure the same spatial area as the US-transducers.

To compensate a strong attenuation of materials a time gain control (TGC) for the RX-E-signals is advisable. RX-T-signals can be used to calculate the attenuation needed for a digital TGC. If one needs to receive quantitative values for a parameter from the echos of a RX-E-transducer it is important to take acoustic shadowing into account. Acoustic shadowing describes the decline of sound energy after a strong reflector or scatterer. A homogeneous TGC cannot take this circumstance into account for quantitative values. We therefore introduced a combined approach with backscatter coefficients. For a time gated echo signal, this approach takes previous traversed gates into account and amplifies rear gates according to the sound energy reaching this gate.

A factor for the reduction of the calculated, used attenu-

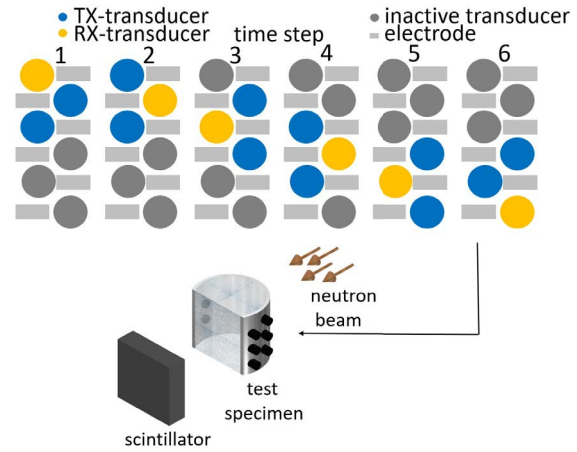


**Figure 1** Excitation scheme for RX-/TX-transducers and experimental setup for determining the liquid fraction in froth with ultrasound. A sequential pulse echo measurement was performed along side with a conductivity measurement. The electrode next to the RX-E-transducer and an opposing one enable a integrative conductivity measurement. The measurement is trained with a conductivity measurement and evaluated with a reference neutron measurement.

ation for TGC can be received in an iterative way. Using a least square algorithm as optimization technique the following steps were repeated with different TGC-factors.

- Customize attenuation for TGC by factor  $x$ .
- Calculating the amplitude envelope of the digitally time gate controlled echo signal.
- Time gating the signal in a desired number of gates and averaging the energy.
- Calculating the backscatter coefficients according to equation 1.
- Determining the best fit of a linear regression with rise zero for the medians of the backscatter coefficients along the gates, as their value should be constant for depth.
- Calculating the least square error between the gates' median and the best fit.

$$b_0 = \frac{RX_0}{I_0} \quad (1a)$$

$$b_n = \frac{RX_n}{I_0 \prod_{i=1}^n (1 - b_{i-1})^2} \quad (1b)$$

Using the optimized parameters, the backscatter coefficients for the desired parameter change are calculated. The range of this change is further on divided into eight bins and a best fit for a linear regression of their medians is conducted.

### 3 Experimental Setup

The described measurement system was integrated into a cylinder as seen in Fig. 1. The cylinder was filled with a SDS-solution (500 ml deionized water, 5 g sodium dodecyl sulfate (SDS)). Needles with diameter 0.59 mm at the bottom of the cylinder enable an air inflow, creating bubbles of  $d_{bubble} = 4$  mm. A peristaltic pump was used to pump solution from the bottom of the cylinder to needles at the top and create a forced drainage in the froth. Using all needles at the top at a constant flow the liquid fraction of the foam was steered to be static and homogeneously distributed. Using only one needle with a time varying flow, also a dynamic inhomogeneous liquid fraction distribution can be achieved. The experiments were conducted at the Paul Scherrer Institut (PSI) in Villigen, Switzerland. The beamline NEUTRA (neutron flux  $> 5 \cdot 10^6$  neutrons  $\cdot cm^{-2} s^{-1} mA^{-2}$  at 25 meV) of the spallation source SINQ [7] was used to receive a reference measurement. Generated reference pictures were corrected according to Carminati et al. [8]

### 4 Measurement Results

Measuring the liquid fraction distribution in froth in two spatial dimensions over time requires a calibration of the measurement system. Two types of validation are being looked at. First the measurement uncertainty in comparison to neutron imaging and second a dynamic inhomogeneous experiment.

#### 4.1 Homogeneous static cases - Calibration

Ten different flow rates of the drainage pump set ten different liquid fractions in the froth. 100 ultrasound scans for each liquid fraction were performed. Due to discrepancies between the electrode measurement and the neutron measurement, the liquid fractions values of each electrode pair were normalized into the range of the corresponding neutron reference. Thus, the measurements are comparable within the resulting liquid fraction range of  $0.17...0.82 \cdot 10^{-2}$ , where 1 signifies pure water.

A classification according to normalized liquid fraction of the electrodes is displayed in Fig. 2. While the medians (white scatter) of the backscatter coefficients rise with increasing liquid fraction by a factor of 10, also the interquartile range (black rectangle) rises by the same factor. Backscatter coefficients greater 0.99 have not been permitted in the optimization process, as it is physically impossible to scatter back more energy than what was introduced. Thus this was a constraint in optimization. For the highest liquid fraction bins outliers (values exceeding the whiskers - horizontal line) over 0.2 and until 0.99 are present but have been cut off in the figure for a clearer presentation. A horizontal end of the violin in the highest liquid fraction appears due to amplified noise. The distributions for the absolute and the relative residuals are depicted at Fig. 3.

An absolute systematic error of  $0.04 \cdot 10^{-2}$  and an absolute random error of  $0.23 \cdot 10^{-2}$  result in an absolute measure-

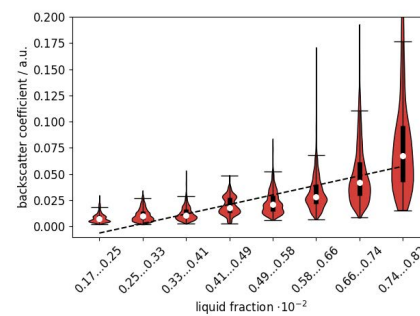


**Figure 2** Violin plot of the backscatter coefficient in different liquid fraction bins. An increase of the backscatter coefficient for higher liquid fractions along with its deviation can be seen. The values of the liquid fraction derive from the conductivity measurement that has been normalized into the range of the reference neutron measurement.

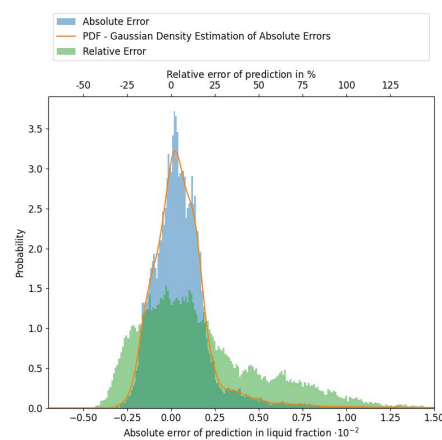


**Figure 3** Histogram of absolute and relative residuals of the liquid fraction estimate and the neutron reference. An absolute and a relative measurement uncertainty of  $0.23 \cdot 10^{-2}$  and 42.5 % have been achieved respectively.

ment uncertainty of  $0.23 \cdot 10^{-2}$  according to the *Guide of Uncertainty of Measurement (GUM)*. The slight overestimation is the result of the error propagation of outliers into the rear gates. The relative error enhances the result of the overestimation. A relative systematic error of 10.7 % and a relative random error of 41.1 % add up to a relative measurement uncertainty of 42.5 %. Outliers for a higher liquid fraction contribute to that increase as well as small absolute errors for small liquid fractions as seen in the first violin in Fig. 2.

#### 4.2 Inhomogeneous dynamic cases - Validation

For a validation, a dynamic and inhomogeneous experiment was carried out. A needle with 75 mm distance to the US-array outputs a volume flow of 10 ml/ min for 11 s. Fig. 4 illustrates the change of liquid fraction over time for the needle positioned above gate five. A running mean over three time points was used to smooth the graphs.

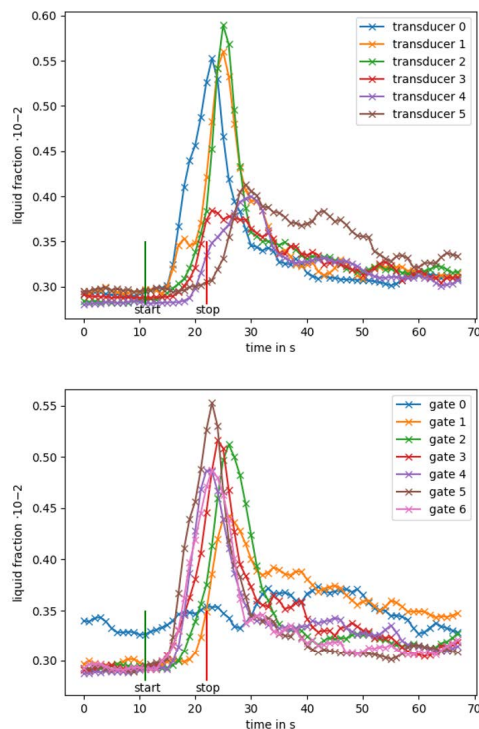


**Figure 4** Estimated liquid fraction over time for the different transducers at gate 5 (upper) and for different gates of Transducer 0 (lower). Transducer 0 signifies the transducer furthest up and closest to the needle, transducer 5 is the bottom transducer, furthest away from the needle. The needle was positioned over gate 5. A rise of liquid fraction can be seen for the different transducers and gates shifting in time and value.

A delay in the peaking liquid fraction as well as a reduced amplitude can be observed for transducers and gates further away from the injection point of liquid fraction change. An image (6x7 pixels) of the liquid fraction distribution with the corresponding reference can be seen in Fig. 5. A convolution with a kernel of size 3x3 for a spatial averaging as well as a temporal smoothing over three time points was applied. The averaged absolute and the relative measurement uncertainty for the liquid fraction estimation is  $0.14 \cdot 10^{-2}$  and 6.42 % respectively. These values match for the filtered and unfiltered data processing.

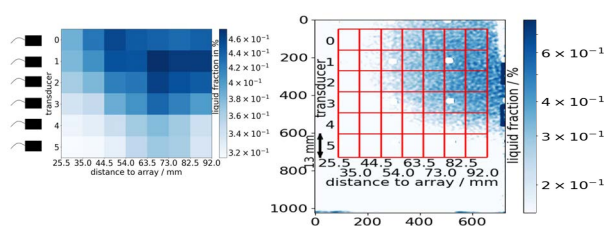


**Figure 5** Image of the liquid fraction distribution. Left is the ultrasound image and on the right the reference neutron image. The ultrasound image was spatially filtered.

## 5 Conclusion

For determining the liquid fraction distribution in liquid foams we build up a measurement system consisting of ultrasound transducers and electrodes. A processing model was derived by a calibration for homogeneous liquid fractions in the range  $0.17 \cdot 10^{-2}$  to  $0.82 \cdot 10^{-2}$ . The measurement in two spatial dimensions (resolution: 13 mm lateral; 7.5 mm axial) and in time (1 Hz) was validated until a penetration depth of 92 mm. Neutron imaging was used as reference measurement to calculate the measurement uncertainty and a dynamic inhomogeneous experiment was conducted to show the application on a use case. Within the analyzed liquid fraction, we have shown for the first time, that a determination of the liquid fraction distribution with ultrasound is possible within the analyzed measurement uncertainties. This represents the first step into advanced process monitoring of flotation processes.

## 6 References

- [1] I. Cantat, S. Cohen-Addad, F. Elias, F. Graner, R. Höhler, O. Pitois, F. Rouyer, and A. Saint-Jalmes, *Foams - Structure and Dynamics*. Oxford University Press, 2010.
- [2] C. Aldrich, C. Marais, B. J. Shean, and J. J. Cilliers, “Online monitoring and control of froth flotation systems with machine vision: A review,” *International Journal of Mineral Processing*, vol. 96, no. 1-4, pp. 1–13, 2010.
- [3] K. Feitosa, S. Marze, A. Saint-Jalmes, and D. J. Durian, “Electrical conductivity of dispersions: From dry foams to dilute suspensions,” *Journal of Physics Condensed Matter*, vol. 17, no. 41, pp. 6301–6305, 2005.
- [4] P. Stevenson, M. D. Matnle, A. J. Sederman, and L. F. Gladden, “Quantitative Measurements of Liquid Holdup and Drainage in Foam Using NMRI,” *AIChE Journal*, vol. 53, pp. 290–296, 2007.
- [5] S. Heitkam, M. Rudolph, T. Lappan, M. Sarma, S. Eckert, P. Trtik, E. Lehmann, P. Vontobel, and K. Eckert, “Neutron imaging of froth structure and particle motion,” *Minerals Engineering*, vol. 119, pp. 126–129, 2018.
- [6] R. Nauber, L. Büttner, K. Eckert, J. Fröhlich, J. Czarske, and S. Heitkam, “Ultrasonic measurements of the bulk flow field in foams,” *Physical Review E*, vol. 97, no. 1, pp. 1–6, 2018.
- [7] <https://www.psi.ch/de/sinq/neutra>, acc. 2021-11-12.
- [8] C. Carminati, P. Boillat, F. Schmid, P. Vontobel, J. Hovind, M. Morgano, M. Raventos, M. Siegwart, D. Mannes, C. Gruenzweig, P. Trtik, E. Lehmann, M. Strobl, and A. Kaestner, “Implementation and assessment of the black body bias correction in quantitative neutron imaging,” *PLoS ONE*, vol. 14, no. 1, pp. 1–24, 2019.